Terahertz absorption spectroscopy study of spin waves in orthoferrite $YFeO_3$ in a magnetic field

K. Amelin,[1] U. Nagel,[1] R. S. Fishman,[2] Y. Yoshida,[3] Hasung Sim,[4,5] Kisoo Park,[4,5] Je-Geun Park,[4,5] and T. Rõõm[1]

[1]*National Institute of Chemical Physics and Biophysics, Tallinn 12618, Estonia*

[2]*Materials Science and Technology Division, Oak Ridge National Laboratory, Oak Ridge, Tennessee 37830, USA*

[3]*National Institute of Advanced Industrial Science and Technology, Tsukuba, Ibaraki 305-8565, Japan*

[4]*Center for Correlated Electron Systems, Institute for Basic Science, Seoul 08826, Korea*

[5]*Department of Physics and Astronomy, Seoul National University, Seoul 08826, Korea*

(Received 4 September 2018; published 14 November 2018)

We measured absorption of THz radiation in $YFeO_3$ single crystals at a temperature of 3 K in the magnetic field up to 17 T applied in all three crystallographic directions. Two spin-wave modes were observed at the Γ point with energies 1.2 meV (9.8 cm^{-1}) and 2.4 meV (19.3 cm^{-1}) in zero field. From the magnetic-field dependence of mode energies, we have refined the previously proposed model [S. E. Hahn *et al.*, Phys. Rev. B **89**, 014420 (2014)] and quantified the parameters of Dzyaloshinskii-Moriya interactions and single-ion anisotropies.

DOI: 10.1103/PhysRevB.98.174417

I. INTRODUCTION

Strong coupling between electric and magnetic orders in multiferroic materials is an interesting phenomenon that allows for tuning of magnetic properties with the applied electric field, and it can find applications in future recording devices and spintronics [1,2]. Such a magnetoelectric effect has been observed in rare-earth orthoferrites R FeO_3, where R is a rare-earth element. $GdFeO_3$, for example, obtains a magnetically induced ferroelectric ground state below 2.5 K, in which the magnetic moment can be controlled with the electric field [3]. The same possibility has been reported [4] for compounds $Dy_{0.7}Tb_{0.3}FeO_3$ and $Dy_{0.75}Gd_{0.25}FeO_3$. While $GaFeO_3$ and $AlFeO_3$ do not belong to the group of rare-earth orthoferrites, their rather similar noncentrosymmetric orthorhombic structure also allows for spontaneous electric polarization and results in multiferroic properties [5].

To fully understand such multiferroic behavior, it is necessary to be able to accurately describe and quantify the interactions inside these materials. Here we focus on an orthoferrite $YFeO_3$ with a distorted perovskite structure of the $Pbnm$ symmetry group. Although the inversion symmetry of this structure does not allow for multiferroicity, $YFeO_3$ is a perfect model system for studying magnetic interactions. In particular, all electron shells in Y^{3+} are completely filled, which means that the magnetic ordering comes exclusively from the Fe^{3+} ions. Thus, modeling this compound allows us to lay the foundation for understanding the magnetoelectric mechanisms and spin dynamics in materials that exhibit more complex behavior.

The striking feature of orthoferrites is their high Néel temperature T_N, which for $YFeO_3$ is reported [6–8] to be approximately 644 K. This property could, in principle, result in room-temperature applications. Below T_N, the iron spins $S = 5/2$ order in an antiferromagnetic (AFM) state $\Gamma_4(G_a, F_c, A_b)$, where the spins are canted, resulting in a weak ferromagnetic (FM) component along the c axis [9,10]. This spin structure is described by a combination of exchange interactions, Dzyaloshinskii-Moriya (DM) interactions that result in weak FM order, and single-ion anisotropies (SIA). It has been shown [11] that with the magnetic field applied along the a axis, the weak FM moment rotates away from the c axis toward the field by 80° at around 7.0 T.

There are four spin-wave (SW) modes associated with the four magnetic ions per unit cell in $YFeO_3$. Two modes have been observed at about 10 and 20 cm^{-1} at the Γ point with Raman spectroscopy [12] and quasioptical techniques [13,14]. Combining these observations with inelastic neutron scattering (INS) measurements of SW dispersion at higher energies led to the development of a simplified spin-state model [15]. There the spin Hamiltonian had two types of exchange interactions (those between nearest-neighbor and next-nearest-neighbor spins), two DM coupling parameters between atoms located in the ab plane, and two SIA constants. From a later structural analysis with INS study of low-energy excitations around a magnetic Brillouin zone center [16], it followed that the model had to be improved by including additional DM interactions between adjacent planes. However, no extensive study of the magnetic-field dependence of SW modes has been performed until now.

The current reexamination of $YFeO_3$ has two motivations. First, THz spectroscopy has far greater sensitivity in frequency than does inelastic neutron scattering. So it is much better suited to study the low-frequency spin dynamics produced by spin-orbit coupling and to estimate the weak, as compared to exchange couplings, DM and SIA interactions in $YFeO_3$. Second, we use this opportunity to incorporate the more complex structure of the DM vectors. By applying

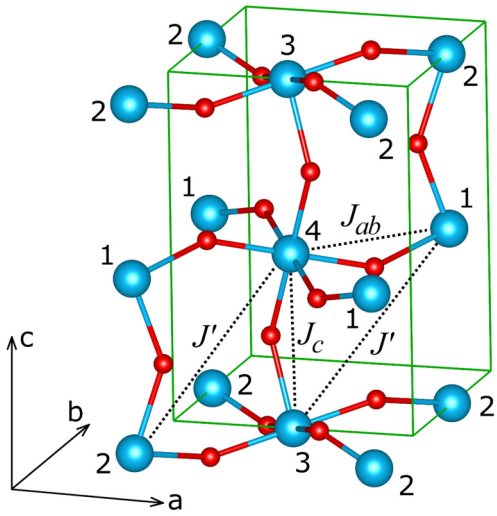

FIG. 1. Magnetic interactions in $YFeO_3$. Magnetic Fe ions are blue and labeled 1 through 4; oxygen ions are red.

the magnetic field in the three crystallographic directions, we obtain much more precise values for the DM and SIA interactions in $YFeO_3$ than was previously possible.

II. THEORY

The magnetic unit cell of $YFeO_3$ contains four $S = 5/2$ Fe^{3+} ions. A sketch of the magnetic unit cell and the exchange interactions between the spins is shown in Fig. 1. We include three exchange interactions: J_{ab} couple pairs of spins $\{1, 4\}$ and $\{2, 3\}$ within the ab plane, J_c couple pairs $\{1, 2\}$ and $\{3, 4\}$ along c, and J' couple pairs $\{1, 3\}$ and $\{2, 4\}$ in different layers separated by $c/2$.

In the absence of DM interactions, the exchange interactions and SIA would stabilize a simple AFM state with spins 1 and 3 aligned along $-\mathbf{a}$ and spins 2 and 4 aligned along $\mathbf{a}$. An earlier work by Hahn *et al.* [15] assumed a simplified model where two DM vectors were taken along $\mathbf{b}$ and $\mathbf{c}$. Each DM interaction was assumed to couple only nearest-neighbor spins, $\{i, j\} = \{2, 3\}$ and $\{1, 4\}$, in the ab plane. The DM vector $\mathbf{D}_2$ then produces the tilt of the spins in the ab plane away from the a axis, and $\mathbf{D}_1$ produces the tilt of the spins toward the c axis [10]. They also included easy-axis SIA K_a and K_c along the a and c axes, respectively. The spin state can be written as

$$\mathbf{S}_i = S(\sin\theta_i \cos\phi_i,\ \sin\theta_i \sin\phi_i,\ \cos\theta_i). \tag{1}$$

In zero field the angles are $\theta_1 = \theta_2 = \theta_3 = \theta_4 \equiv \theta$ and $\phi_1 + \pi = -\phi_3 + \pi = -\phi_4 = \phi_2 \equiv \phi$. This state has a net spin c-component $F_c = (\mathbf{S}_1 + \mathbf{S}_2 + \mathbf{S}_3 + \mathbf{S}_4)_c = 4S\cos\theta$ per magnetic unit cell. It has no spin component perpendicular to the c axis, but it has AF components along the a axis, $G_a = (\mathbf{S}_1 - \mathbf{S}_2 + \mathbf{S}_3 - \mathbf{S}_4)_a$, and the b axis, $A_b = (\mathbf{S}_1 - \mathbf{S}_2 - \mathbf{S}_3 + \mathbf{S}_4)_b$. The relations between spin vectors and angles are $A_b/G_a = \tan\phi$ and $F_c/G_a = (\cos\phi\tan\theta)^{-1}$.

Hahn *et al.* [15] fit the SW spectrum to obtain the exchange interactions, SIA, and DM vectors. The set of parameters was constrained to produce the zero-field spin state with $\theta = 0.498\pi$ and $\phi = 0.001\pi$. Because J_{ab} and J_c couple sites that are bridged by one anion and separated by distances $\sqrt{a^2 + b^2}/2 \approx 3.85$ Å and $c/2 \approx 3.80$ Å, respectively, these two antiferromagnetic coupling constants were set equal to the single exchange constant J. By contrast, J' couples sites that are bridged by two anions and by distance $\sqrt{a^2 + b^2 + c^2}/2 \approx 5.41$ Å. So $|J'|$ is expected to be much smaller than $|J|$. Hahn *et al.* estimated that $J = -4.77$ meV and $J' = -0.21$ meV. The SIA $K_a = 0.0055$ meV and $K_c = 0.0035$ meV favor the spins to lie perpendicular to the b axis. The DM vectors had estimated magnitudes $D_1 = 0.074$ meV and $D_2 = 0.028$ meV.

However, a symmetry analysis of the perovskite crystal structure [17] revealed that the DM vectors are more complex than assumed by Hahn *et al.* [15]. Rather than just two DM vectors, each oxygen atom-mediated bond (Fig. 1) carries its own local DM vector, including nearest neighbors $\{1, 2\}$ and $\{3, 4\}$ on adjacent ab planes separated by $\pm c/2$. While there are still only two overall magnitudes for the DM vectors, this more complex interaction structure could modify the estimates for the microscopic parameters in $YFeO_3$.

With the magnetic field $\mathbf{H}$ along $\mathbf{m}$, the Hamiltonian of $YFeO_3$ can be written as

$$\begin{aligned}\mathcal{H} = &-\frac{1}{2}J\sum_{i,j}\mathbf{S}_i\cdot\mathbf{S}_j - \frac{1}{2}J'\sum_{i,j}\mathbf{S}_i\cdot\mathbf{S}_j \\ &- K_a\sum_i {S_{ia}}^2 - K_c\sum_i {S_{ic}}^2 \\ &+ \frac{1}{2}\sum_{i,j}\mathbf{D}_{ij}\cdot(\mathbf{S}_i\times\mathbf{S}_j) - \mu_B\mu_0 H\sum_i \mathbf{m}\cdot\mathbf{S}_i,\end{aligned} \tag{2}$$

where the exchange interactions couple the spins indicated in Fig. 1, and $J_{ab} = J_c \equiv J$. The factors of $1/2$ avoid double counting. Because the spectroscopic modes are evaluated at wave vector $\mathbf{q} = \mathbf{0}$, we do not include interactions between spins in neighboring unit cells, e.g., between $\mathbf{S}_1$ and $\mathbf{S}_1$, although these are next-nearest-neighbor interactions.

The orientation of the local vectors $\mathbf{D}_{ij}$ is determined by the condition that [18]

$$\mathbf{D}_{ij} \propto (\mathbf{R}_i - \mathbf{R}_o)\times(\mathbf{R}_o - \mathbf{R}_j), \tag{3}$$

where $\mathbf{R}_o$ is the position of the oxygen atom that couples spins i and j. Consequently, the DM vectors are given by [17]

$$\mathbf{D}_{32} = D_{ab}(-\alpha_{ab}, \beta_{ab}, \gamma_{ab}),\ \Delta\mathbf{R} = \pm(a/2, b/2, 0), \tag{4}$$

$$\mathbf{D}'_{32} = D_{ab}(\alpha_{ab}, \beta_{ab}, \gamma_{ab}),\ \Delta\mathbf{R} = \pm(-a/2, b/2, 0), \tag{5}$$

$$\mathbf{D}_{41} = D_{ab}(-\alpha_{ab}, -\beta_{ab}, \gamma_{ab}),\ \Delta\mathbf{R} = \pm(-a/2, b/2, 0), \tag{6}$$

$$\mathbf{D}'_{41} = D_{ab}(\alpha_{ab}, -\beta_{ab}, \gamma_{ab}),\ \Delta\mathbf{R} = \pm(a/2, b/2, 0), \tag{7}$$

$$\mathbf{D}_{12} = D_c(-\alpha_c, \beta_c, 0),\ \Delta\mathbf{R} = \pm(0, 0, c/2), \tag{8}$$

$$\mathbf{D}_{34} = D_c(\alpha_c, \beta_c, 0),\ \Delta\mathbf{R} = \pm(0, 0, c/2), \tag{9}$$

where $\Delta\mathbf{R} = \mathbf{R}_i - \mathbf{R}_j$ for $\mathbf{D}_{ij} = -\mathbf{D}_{ji}$. The vectors are all normalized so that $\alpha_{ab}^2 + \beta_{ab}^2 + \gamma_{ab}^2 = 1$ and $\alpha_c^2 + \beta_c^2 = 1$.

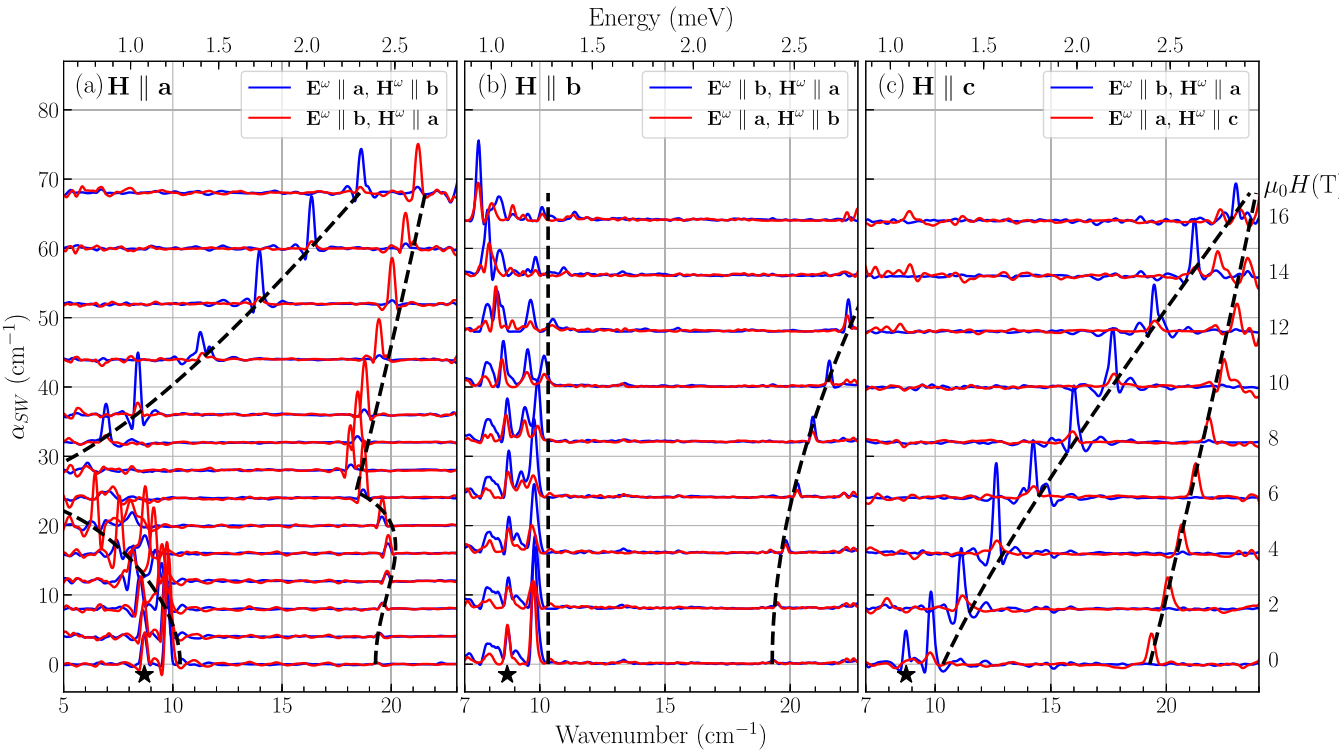

FIG. 2. Magnetic-field dependence of SW absorption spectra of $YFeO_3$ at 3 K. Panels (a), (b), and (c) correspond to the magnetic field **H** applied along crystallographic axes a, b, and c, respectively. The spectra are shifted vertically in proportion to the magnitude of the applied magnetic field, marked on the right side of the plot. In each panel, blue and red solid lines denote two orthogonal incident light polarizations, where the oscillating electric- and magnetic-field vectors $\mathbf{E}^\omega$ and $\mathbf{H}^\omega$ are aligned along different crystallographic axes. Dashed lines show the absorption peak positions obtained from the theoretical fit. The impurity peak position in zero field is marked with a star.

Based on Eq. (3) and the structural analysis [16], $\alpha_{ab} = 0.517$, $\beta_{ab} = 0.488$, $\gamma_{ab} = 0.703$, $\alpha_c = 0.346$, and $\beta_c = 0.938$.

III. EXPERIMENT

We prepared polycrystalline $YFeO_3$ using Y_2O_3 and Fe_2O_3 by a standard solid-state reaction method. All the starting materials were prepared in a stoichiometric ratio and mixed, pelletized, and sintered several times. The final sintering condition was set to 1400 °C for 24 h. Single crystals were subsequently grown with a 4-mm-diameter feed rod of a correct composition by a floating-zone furnace (Crystal Systems, Japan) under an oxygen atmosphere at a growth speed of 3 mm/h. We checked the quality of the samples using a single-crystal diffractometer and bulk property measurements.

Three cuts of $YFeO_3$ single crystals, (100), (010), and (001), with thicknesses slightly under 1 mm were prepared. The intensity of transmitted THz radiation was detected in the range from 5 to 40 cm^{-1} using a Martin-Puplett interferometer, a mercury discharge lamp as a light source, and a Si bolometer operated at $T = 0.3$ K. The polarization of incident radiation was controlled by a wire-grid polarizer. Measurements were performed in Faraday and Voigt configurations, where the THz radiation propagates parallel or perpendicular to the applied magnetic field, respectively. In a Voigt configuration, the SW mode frequencies were measured as a function of the sample orientation in fields just below and above the observed spin-flop (SF) transition (i.e., 5 and 7 T). The sample was rotated around the c axis such that the magnetic-field vector was in the ab plane. The exact alignment $\mathbf{H} \parallel \mathbf{a}$ was achieved by finding the orientation that corresponds to the lowest frequency of the resonance peak.

Differential absorbance spectra were calculated from the ratios of transmitted light intensities measured with and without the applied magnetic field in the following way. In a sample with negligible interference (i.e., wedged or with high enough absorption), the transmitted light intensity I is related to the incident light intensity I_0 via $I = I_0(1-R)^2\exp(-\alpha d)$, where R is the reflection coefficient, α is the absorption coefficient, and d is the sample thickness. Therefore, the absorption coefficient is defined as $\alpha = -d^{-1}\ln[(1-R)^{-2}I/I_0]$. If we assume that R does not depend on the applied magnetic field, we can calculate the differential absorbance $\alpha_{\mathrm{SW}} \equiv \alpha(H) - \alpha(0) = -d^{-1}\ln[I(H)/I(0)]$ by dividing the transmitted intensity spectrum measured in the magnetic field $I(H)$ by the zero-field spectrum $I(0)$. Finally, a baseline, statistically calculated from negative values of α_{SW}, is subtracted to reveal absorption peaks in the zero-field spectrum.

IV. RESULTS

Using THz spectroscopy, we have measured two lowest spin-wave modes at $\mathbf{q} = \mathbf{0}$ for the magnetic field along the a, b, and c axes, with results shown in Fig. 2. $YFeO_3$ undergoes a spin-flop transition when the field is applied along the a axis. While the spins are almost parallel to the a axis below H_{SF}, they are almost parallel to the c axis above H_{SF}.

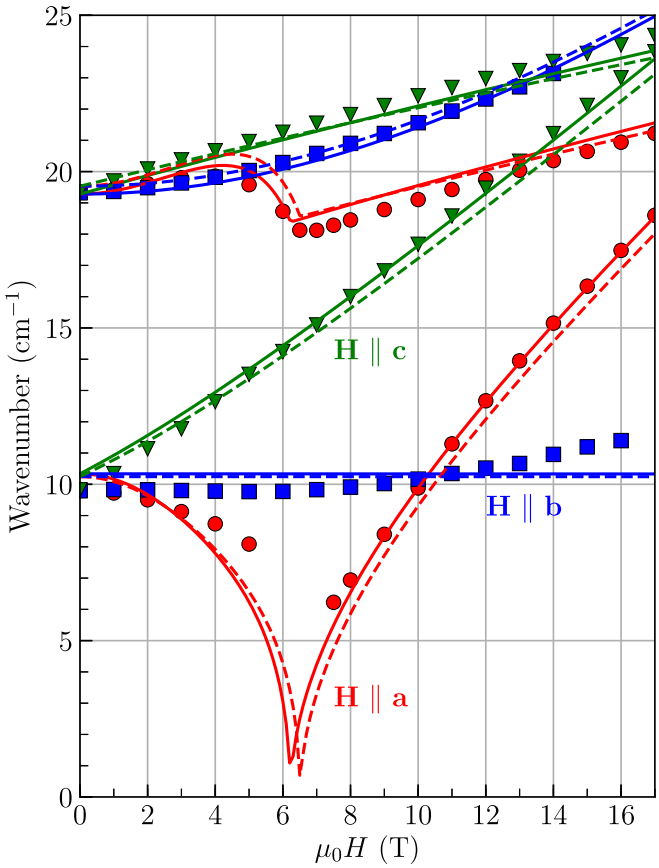

FIG. 3. Magnetic-field dependence of the absorption peak positions (symbols) with the field applied along the three crystallographic axes and the theoretical fit result (solid lines). Dashed lines show the fit with the simplified model, where $D_c = 0$.

In addition to the two SW modes, there exists another mode below 9 cm^{-1}, which is especially pronounced in Figs. 2(a) and 2(b), and it has been indicated with a star. This mode has previously been reported [19,20] to be an impurity mode only present in single crystals grown by the floating zone method. The mode was assigned to Fe^{3+} atoms occupying Y^{3+} sites, and is not accounted for in the present model.

Since THz spectroscopy only measures the two low-frequency modes below 3 meV, we use the SW spectrum measured with INS [15] for frequencies up to 80 meV to fix the exchange interactions $J_c = J_{ab} = -4.77$ meV and $J' = -0.21$ meV. That leaves the four "small" spin-orbit parameters K_a, K_c, D_{ab}, and D_c to be determined by optical spectroscopy.

For each field direction and magnitude and set of parameters, we minimize the energy $E = \langle \mathcal{H} \rangle$ as a function of the eight angles θ_i and ϕ_i for the four spins in the magnetic unit cell. Based on the linear SW theory, we then evaluate the frequencies of the two lowest SW modes for comparison with the measured spectroscopic mode frequencies. This loop is repeated until we achieve a minimum of χ^2.

The result of this procedure is presented in Fig. 3, which shows a rather good agreement between the theory and the experimental data. All of the coupling parameters are summarized in Table I, where the values are compared to those from

TABLE I. Spin Hamiltonian parameter values (meV). The two DM parameters of Hahn *et al.* [15] are related to D_{ab} as $D_{ab} = \sqrt{D_1^2 + D_2^2}$.

	This work	$D_c = 0$	Hahn *et al.* [15]	Park *et al.* [16]
J_c	−4.77	−4.77	−4.77	−5.02
J_{ab}	−4.77	−4.77	−4.77	−4.62
J'	−0.21	−0.21	−0.21	−0.22
K_a	0.0052	0.0055	0.0055	0.0091
K_c	0.0044	0.0038	0.0031	0.0025
$\lvert D_{ab} \rvert$	0.136	0.147	0.079	0.121
$\lvert D_c \rvert$	0.189	0		0.145

earlier reports. The resulting values of K_a and K_c are quite close to those predicted by Hahn *et al.* [15]. Not surprisingly, considering that the DM vectors are oriented away from the c and b axes, the values for D_{ab} and D_c are larger than $\sqrt{D_1^2 + D_2^2}$ estimated by Hahn *et al.* [15]. These parameters correspond to the zero-field canted state with $\theta = 0.4966\pi$ and $\phi = 0.0035\pi$, which is more canted than previously predicted. When the field is applied along the a axis, these parameters produce a SF field $\mu_0 H_{SF} = 6.2$ T.

We evaluated the validity of the more complex DM model by also fitting the experimental data using a simplified model from Hahn *et al.* [15], with $D_c = 0$ and $\alpha_{ab} = 0$. In this case the four fitting parameters are D_1, D_2, K_a, and K_c. The result is plotted in Fig. 3 with dashed lines. While it is still possible to fit the spectrum rather well with fixed $D_c = 0$, it does not match the experimental data as closely as the more complex model that includes DM interaction between adjacent planes. This is confirmed by the difference in χ^2 (0.462 against 0.168). The corresponding fit parameters are specified in Table I in the second column. The values of D_1 and D_2 are 0.139 and 0.048 meV, respectively.

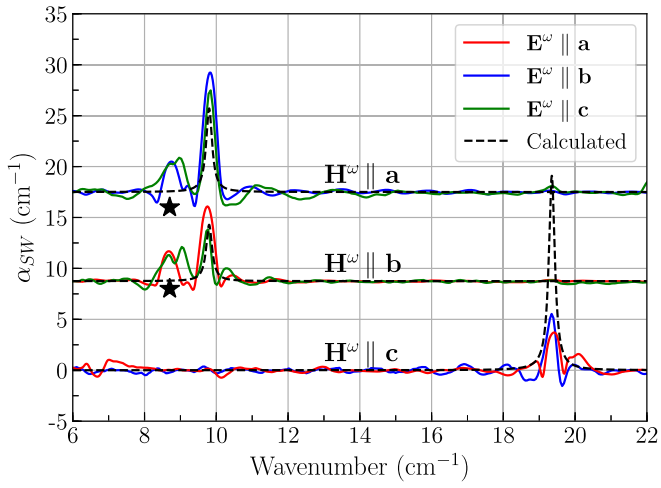

FIG. 4. Zero-field spectra measured in six different polarizations qualitatively showing the selection rules. The spectra are grouped according to the direction of the oscillating magnetic field $\mathbf{H}^\omega$. For each direction, only one mode is visible. The dashed lines show arbitrarily scaled theoretical spectra. The impurity mode is marked with a star.

Figure 4 qualitatively shows the selection rules for $YFeO_3$. It is clear that the absorption intensity depends on the direction of the oscillating magnetic field $\mathbf{H}^{\omega}$ rather than the electric field $\mathbf{E}^{\omega}$. The selection rules are well reproduced by the theory, where in zero field the lower-frequency mode is visible in polarizations with $\mathbf{H}^{\omega} \parallel \mathbf{a}$ and $\mathbf{H}^{\omega} \parallel \mathbf{b}$, while the higher-frequency mode occurs exclusively with $\mathbf{H}^{\omega} \parallel \mathbf{c}$. While the theory qualitatively matches the experiment in the whole magnetic-field range (selection rules change after the spin flop), we have not been able to accurately reproduce the absorption intensities. Thus, in Fig. 4 the higher-frequency mode is predicted to have much higher intensity, while in reality the intensities of the two modes are comparable. The cause of this discrepancy remains unknown.

V. CONCLUSION

Two SW modes were measured by THz absorption spectroscopy and modeled by the Hamiltonian, Eq. (2). Our result shows that it is necessary to account for the more complex DM structure to accurately model the magnetic interactions in $YFeO_3$, which is confirmed by the overall quality of the fits. With that in mind, we were able to fit the magnetic-field dependence of the absorption spectra up to 17 T, from which we precisely quantified the SIA and DM interactions. These values are in good agreement with earlier reported INS data, and are only slightly modified.

The obtained canting, with angles $\theta = 0.4966\pi$ and $\phi = 0.0035\pi$, is considerably larger than that previously reported by Hahn *et al.* [15] (0.4983π and 0.0010π) and is very close to what was estimated by Park *et al.* [16] (0.4972π and 0.0032π). This larger canting results from the higher magnitudes of the DM interaction vectors than previously predicted. The new values of canting angles correspond better to the experimentally observed [10] ratios $F_c/G_a = 0.0129$ and $A_b/G_a = 0.0159$ that correspond to $\theta = 0.4959\pi$ and $\phi = 0.0051\pi$.

It is worth noting that the spin flop occurs at $\mu_0 H_{SF} = 6.2$ T with the current set of parameters, which is lower than the previously reported value of 7.0 T. Unfortunately, it is hard to unambiguously determine the exact SF field from the experimental data alone, as the lower SW mode does not soften completely. Why does the lower, experimental mode frequency not soften as much as predicted near H_{SF}? There might be several explanations for this discrepancy. SW theory does not include higher-order fluctuations that could enhance the SW frequencies near H_{SF}. Because the predicted drop in the lowest mode frequency is very steep, it will be significantly lifted by crystal domains with slightly different spin-flop fields. However, 6.2 T clearly matches the SF field we observed much better than what is estimated using sets of parameters from Hahn *et al.* [15] or Park *et al.* [16], which is 9.0 and 15.9 T, respectively. This is a good indication that fitting the magnetic-field dependence of THz spectra provides a better estimation of the SIA and DM interaction parameters.

Therefore, we have shown that while INS is better suited to estimate the stronger exchange couplings based on the SW dispersion at high frequencies, THz spectroscopy is better suited to study the "weak" spin-orbit induced DM and SIA couplings at low frequencies and $\mathbf{q} = \mathbf{0}$. Since these "weak" interactions are responsible for a material's multiferroic behavior, THz spectroscopy should prove useful in the future, when this approach is extended to materials where Y^{3+} is substituted by other, possibly magnetic ions.

One of the challenges of our method is currently the limited availability of large enough high-quality single crystals for transmission measurements. The other limitation is the fact that we cannot very well detect low-frequency modes that soften close to the spin flop, as it is hard to measure below 5 cm^{-1} with THz spectroscopy. While we are currently not able to determine the cause of the discrepancy between the theoretical and the measured absorption intensities, we hope to find the answer in future measurements that would include other orthoferrites.

ACKNOWLEDGMENTS

We would like to thank R. K. Kremer and M. Krautloher from Max-Planck Institute for Solid State Research in Stuttgart for providing assistance with x-ray and Laue measurements. Special thanks to D. Hüvonen, J. Viirok, and L. Peedu for the help with THz measurements in Tallinn. We acknowledge support of the Estonian Ministry of Education and Research with institutional research funding IUT23-3, and the European Regional Development Fund Project No. TK134 (K.A., T.R., and U.N.). Research sponsored by the U.S. Department of Energy, Office of Basic Energy Sciences, Materials Sciences and Engineering Division (R.S.F.).

[1] S. M. Wu, S. A. Cybart, P. Yu, M. D. Rossell, J. X. Zhang, R. Ramesh, and R. C. Dynes, Nat. Mater. **9**, 756 (2010).
[2] C. Binek and B. Doudin, J. Phys.: Condens. Matter **17**, L39 (2005).
[3] Y. Tokunaga, N. Furukawa, H. Sakai, Y. Taguchi, T. Arima, and Y. Tokura, Nat. Mater. **8**, 558 (2009).
[4] Y. Tokunaga, Y. Taguchi, T. Arima, and Y. Tokura, Nat. Phys. **8**, 838 (2012).
[5] R. Saha, A. Shireen, S. N. Shirodkar, U. V. Waghmare, A. Sundaresan, and C. N. R. Rao, Solid State Commun. **152**, 1964 (2012).
[6] V. M. Judin, A. B. Sherman, and I. E. Myl'nikova, Phys. Lett. **22**, 554 (1966).
[7] H. Shen, J. Xu, A. Wu, J. Zhao, and M. Shi, Mater. Sci. Eng., B **157**, 77 (2009).
[8] D. Treves, J. Appl. Phys. **36**, 1033 (1965).
[9] D. Treves, Phys. Rev. **125**, 1843 (1962).
[10] V. P. Plakhty, Y. P. Chernenkov, and M. N. Bedrizova, Solid State Commun. **47**, 309 (1983).
[11] J. Scola, Y. Dumont, N. Keller, M. Vallée, J.-G. Caputo, I. Sheikin, P. Lejay, and A. Pautrat, Phys. Rev. B **84**, 104429 (2011).

[12] R. M. White, R. J. Nemanich, and C. Herring, Phys. Rev. B **25**, 1822 (1982).
[13] A. A. Volkov, Y. G. Goncharov, G. V. Kozlov, S. P. Lebedev, and A. M. Prokhorov, Infr. Phys. **25**, 369 (1985).
[14] A. A. Mukhin, A. N. Lobanov, and M. Gorian, J. Magn. Res. **195**, 60 (2008).
[15] S. E. Hahn, A. A. Podlesnyak, G. Ehlers, G. E. Granroth, R. S. Fishman, A. I. Kolesnikov, E. Pomjakushina, and K. Conder, Phys. Rev. B **89**, 014420 (2014).
[16] K. Park, H. Sim, J. C. Leiner, Y. Yoshida, J. Jeong, S. Yano, J. Gardner, P. Bourges, M. Klicpera, V. Sechovský, M. Boehm, and J.-G. Park, J. Phys.: Condens. Matter **30**, 235802 (2018).
[17] M. Mochizuki and N. Furukawa, Phys. Rev. B **80**, 134416 (2009).
[18] F. Keffer, Phys. Rev. **126**, 896 (1962).
[19] A. M. Balbashov, A. G. Berezin, J. V. Bobryshev, P. J. Marchukov, I. V. Nikolaev, E. G. Rudashevsky, J. Paches, and L. Půst, J. Magn. Magn. Mater. **104-107**, 1037 (1992).
[20] A. M. Balbashov, G. V. Kozlov, A. A. Mukhin, and A. S. Prokhorov, in *High Frequency Processes in Magnetic Materials*, edited by G. Srinivasa and A. N. Slavin (World Scientific, Singapore, 1995), Chap. 2, pp. 56–98.